African Journal of Mathematics and Computer Science Research Vol. 2(9), pp. 189-195, October, 2009
Available online at http://www.academicjournals.org/AJMCSR ISSN 2006-9731

Full Length Research Paper

Comparison of electron-plasmon scattering effect on low-field electron mobility in ZnO and SiC

H. Arabshahi* and M. Rezaee Rokn-Abadi

Physics Department, Ferdowsi University of Mashhad, Mashhad, Iran.

Accepted 8 September, 2009

Iterative technique is used to solve Boltzmann transport equation for calculating temperature and doping dependencies of electron mobility in ZnO and SiC materials. The two-mode nature of the polar optic phonons is considered jointly with deformation potential acoustic, piezoelectric, ionized impurity and electron-plasmon scattering. Band non-parabolicity, admixture of *p* functions, arbitrary degeneracy of the electron distribution, and the screening effects of free carriers on the scattering probabilities are incorporated. It is shown that electron-plasmon scattering affects substantially the low-field electron mobility in bulk ZnO and SiC. It is found that the electron mobility decreases monotonically as the temperature increases from 300 - 600 K. The low temperature value of electron mobility increases significantly with increasing doping concentration. The iterative results are in fair agreement with other recent calculations obtained using the relaxation-time approximation and experimental methods.

Key words: Electron-plasmon, relaxation-time, Boltzmann equation, non-parabolicity, degeneracy.

INTRODUCTION

Zinc oxide and sillicon carbide are of potential interest as a suitable materials for high temperature, high power electronic devices either as the active material or as a suitable substrate for epitaxial growth of group III-nitride compounds (Hamdani, 1997). Prior to advances in vapor-phase growth yielding high quality bulk of ZnO and SiC cystals [Look, 2005]; practical applications for these materials were limited to those requiring only oriented ploycrystallities or powder [Kim, 1999]. With those large, direct band gap and wurtzite crystal structure, ZnO and SiC are similar to GaN. Furthermore, due to its relatively close match in lattice constants, it may be used as a substrate for GaN and AlN epitaxy (Tsukazaki et al., 2005). As a consequence, there is renewed interest in the properties of ZnO and SiC relevant for device applications (Makino et al., 2001). The low-field electron mobility is one of the most important parameters that determine the performance of a field-effect transistor. The purpose of the present paper is to calculate electron mobility for various temperatures and ionized-impurity concentrations. The formulation itself applies only to the central Γ valley conduction band. We have also consider band non-parabolicity, admixture of *p*- type valence-band wave functions, degeneracy of the electron distribution to any arbitrary degree, and the screening effects of free carriers on the scattering probabilities [Bellotti et al., 1999]. All the relevant scattering mechanisms, including the two-mode nature of the polar optic phonon and electron-plasmon scattering are taken into account. The Boltzmann equation is solved iteratively for our purpose, jointly incorporating the effects of all the scattering mechanisms [Look et al., 1998]. Our calculated results are compared with the available experimental data on both temperature and the free electron concentration dependence of mobility [Chen et al., 1998].

This paper is organized as follows. Details of the iterative model, the electron scattering mechanism which have been used and the electron mobility calculations are presented in section 2 and the results of iterative calculations carried out on ZnO structure are interpreted in section 3.

MODEL DETAILS

To calculate mobility, we have to solve the Boltzmann equation to get the modified probability distribution function under the action of a steady electric field. Here we have adopted the iterative technique for solving the Boltzmann transport equation. Under the action of a

---

*Corresponding author. E-mail: arabshahi@um.ac.ir.

steady field, the Boltzmann equation for the distribution function can be written as

$$\frac{\partial f}{\partial t}+v.\nabla_r f+\frac{eF}{\hbar}.\nabla_k f=\left(\frac{\partial f}{\partial t}\right)_{coll} \qquad (1)$$

Where *(∂ f/∂ t)*$_{coll}$ represents the change of distribution function due to the electron scattering. In the steady-state and under application of a uniform electric field the Boltzmann equation can be written as

$$\frac{eF}{\hbar}.\nabla_k f=\left(\frac{\partial f}{\partial t}\right)_{coll} \qquad (2)$$

Consider electrons in an isotropic, non-parabolic conduction band whose equilibrium Fermi distribution function is $f_0(k)$ in the absence of electric field. Note the equilibrium distribution $f_0(k)$ is isotropic in k space but is perturbed when an electric field is applied. If the electric field is small, we can treat the change from the equilibrium distribution function as a perturbation which is first order in the electric field. The distribution in the presence of a sufficiently small field can be written quite generally as

$$f(k)=f_0(k)+f_1(k)\cos\theta \qquad (3)$$

Where θ is the angle between k and F and $f_1(k)$ is an isotropic function of k, which is proportional to the magnitude of the electric field. $f(k)$ satisfies the Boltzmann equation 2 and it follows that:

$$\frac{eF}{\hbar}\frac{\partial f_0}{\partial t}=\sum_i\left\{\int\cos\varphi f_1'\left[s_i'(1-f_0)+s_i f_0\right]d^3k'-f_1\int\left[s_i(1-f_0')+s_i'f_0'\right]d^3k'\right\} \qquad (4)$$

In general there will be both elastic and inelastic scattering processes. For example impurity scattering is elastic and acoustic and piezoelectric scattering are elastic to a good approximation at room temperature. However, polar and non-polar optical phonon scattering are inelastic. Labeling the elastic and inelastic scattering rates with subscripts *el* and *inel* respectively and recognizing that, for any process *i*, $s_{eli}(k', k) = s_{eli}(k, k')$ equation 4 can be written as

$$f_1(k)=\frac{\frac{-eF}{\hbar}\frac{\partial f_0}{\partial k}+\sum\int f_1'\cos\varphi[s_{inel}'(1-f_0)+s_{inel}f_0)]d^3k'}{\sum\int(1-\cos\varphi)s_{el}d^3k'+\sum\int[s_{inel}(1-f_0')+s_{inel}'f_0']d^3k'} \qquad (5)$$

Note the first term in the denominator is simply the momentum relaxation rate for elastic scattering. Equation 5 may be solved iteratively by the relation

$$f_{1n}(k)=\frac{\frac{-eF}{\hbar}\frac{\partial f_0}{\partial k}+\sum\int f_1(k')[n-1]\cos\varphi[s_{inel}'(1-f_0)+s_{inel}f_0)]d^3k'}{\sum\int(1-\cos\varphi)s_{el}d^3k'+\sum\int[s_{inel}(1-f_0')+s_{inel}'f_0']d^3k'} \qquad (6)$$

Where f_{1n} (*k*) is the perturbation to the distribution function after the *n*-th iteration. It is interesting to note that if the initial distribution is chosen to be the equilibrium distribution, for which f_1 (*k*) is equal to zero, we get the relaxation time approximation result after the first iteration. We have found that convergence can normally be achieved after only a few iterations for small electric fields. Once f_1 (*k*) has been evaluated to the required accuracy, it is possible to calculate quantities such as the drift mobility μ, which is given in terms of spherical coordinates by

$$\mu=\frac{\hbar}{3m^*F}\frac{\int_0^\infty(k^3/1+2\alpha F)f_1d^3k}{\int_0^\infty k^2f_0d^3k} \qquad (7)$$

Here, we have calculated low field drift mobility in ZnO and SiC structures using the iterative technique. In the following sections electron-phonon electron-impurity, and electron-plasmon scattering mechanisms will be discussed.

Deformation potential scattering

The acoustic modes modulate the inter atomic spacing. Consequently, the position of the conduction and valence band edges and the energy band gap will vary with position because of the sensitivity of the band structure to the lattice spacing. The energy change of a band edge due to this mechanism is defined by a deformation potential and the resultant scattering of carriers is called deformation potential scattering. The energy range involved in the case of scattering by acoustic phonons is from zero to $2\hbar vk$, where v is the velocity of sound, since momentum conservation restricts the change of phonon wave vector to between zero and 2*k*, where *k* is the electron wave vector. Typically, the average value of k is of the order of 10^7 cm^{-1} and the velocity of sound in the medium is of the order of 10^5 cms^{-1}. Hence, $2\hbar vk$ ~ 1 meV, which is small compared to the thermal energy at room temperature. Therefore, the deformation potential scattering by acoustic modes can be considered as an elastic process except at very low temperature. The deformation potential scattering rate with either phonon emission or absorption for an electron of energy *E* in a non-parabolic band is given by Fermi's golden rule as [Moglestue, 1993; Jacoboni, 1989]

$$R_{de}(k)=\frac{\sqrt{2}D_{ac}^2(m_t^{*2}m_l^*)^{1/2}K_BT}{\pi\rho v^2\hbar^4}\frac{\sqrt{E(1+\alpha E)}}{(1+2\alpha E)}\left[(1+\alpha E)^2+1/3(\alpha E)^2\right] \qquad (8)$$

Where D_{ac} is the acoustic deformation potential, ρ is the material density and α is the non-parabolicity coefficient. The formula clearly shows that the acoustic scattering increases with temperature.

Piezoelectric scattering

The second type of electron scattering by acoustic modes occurs when the displacements of the atoms create an electric field through the piezoelectric effect. This can occur in the compound semiconductors such as the III-V and II-VI materials including ZnO and SiC which in fact have a relatively large piezoelectric constant. The piezoelectric scattering rate for an electron of energy *E* in an isotropic, parabolic band has been discussed by Ridley [Ridley, 1997] who included the modification of the Coulomb potential due to free carrier screening. The screened Coulomb potential is written as

$$V(r) = \frac{e^2}{4\pi\varepsilon_0\varepsilon_s}\frac{\exp(-q_0 r)}{r} \tag{9}$$

Where ε_s is the relative dielectric constant of the material and q_0 is the inverse screening length, which under non-degenerate conditions is given by

$$q_0^2 = \frac{ne^2}{\varepsilon_0\varepsilon_s K_B T} \tag{10}$$

Where *n* is the electron density. The expression for the scattering rate of an electron in a non-parabolic band structure retaining only the important terms can be written as [Moglestue, 1993; Jacoboni, 1989]:

$$R_{pz}(k) = \frac{\sqrt{m^*}\,e^2 K_{av}^2 K_B T}{4\sqrt{2}\pi\hbar^2\varepsilon_0\varepsilon_s}\gamma^{-1/2}(E)(1+2\alpha E)^2 \times \left[\ln(1+\frac{8m^*\gamma(E)}{\hbar^2 q_0^2}) - \frac{1}{1+\hbar^2 q_0^2/8m^*\gamma(E)} + \left(\frac{\sqrt{2}\alpha E}{1+2\alpha E}\right)^2\right] \tag{11}$$

Where K_{av} is the dimensionless so called average electromechanical coupling constant.

Polar optical phonon scattering

The dipolar electric field arising from the opposite displacement of the negatively and positively charged atoms provides a coupling between the electrons and the lattice which results in electron scattering. This type of scattering is called polar optical phonon scattering and at room temperature is generally the most important scattering mechanism for electrons in III-V semiconductors, and this is also the case in ZnO and SiC despite the fact that the optical phonon energy is particularly high at ~ 93 meV which suppresses the phonon population and also electrons must reach that energy before phonon emission is possible. The scattering rate due to this process for an electron of energy *E* in an isotropic, non-parabolic band is (Moglestue, 1993; Jacoboni, 1989)

$$R_{po}(k) = \frac{\sqrt{2m^*}\,e^2\omega_{op}}{8\pi\varepsilon_0\hbar}(\frac{1}{\varepsilon_\infty} - \frac{1}{\varepsilon_s})\frac{1+2\alpha E'}{\gamma^{1/2}(E)} \times F_0(E,E')\{N_{op}, N_{op}+1\} \tag{12}$$

Where N_{op} is the phonon occupation number and the upper and lower cases refer to absorption and emission, respectively. For small electric fields, the phonon population will be very close to equilibrium so that the average number of phonons is given by the Bose-Einstein distribution.

Non-polar optical phonon scattering

Non-polar optical phonon scattering is similar to deformation potential scattering, in that the deformation of the lattice produces a perturbing potential but in this case the deformation is carried by optical vibrations. The non-polar optical phonon scattering rate in non-parabolic bands is given by [Moglestue, 1993; Jacoboni, 1989]

$$R_{npo}(k) = \frac{D_{od}^2 (m_t^{*2} m_l^*)^{1/2}}{\sqrt{2}\pi\hbar^3\rho\omega_{op}}(1+2\alpha E)\gamma^{1/2}(E)\left[N_{op}, N_{op}+1\right] \tag{13}$$

Where D_{od} is the optical deformation potential and $E = E' \pm \hbar\omega_{op}$ is the final state energy phonon absorption (upper case) and emission (lower case).

Impurity scattering

This scattering process arises as a result of the presence of impurities in a semiconductor. The substitution of an impurity atom on a lattice site will perturb the periodic crystal potential and result in scattering of an electron. Since the mass of the impurity greatly exceeds that of an electron and the impurity is bonded to neighboring atoms, this scattering is very close to being elastic. Ionized impurity scattering is dominant at low temperatures because, as the thermal velocity of the electrons decreases, the effect of long-range Coulombic interactions on their motion is increased. The electron scattering by ionized impurity centres has been discussed by Brooks-

Herring (Chattopadhyay, 1981) who included the modification of the Coulomb potential due to free carrier screening. The scattering rate for an isotropic, non-parabolic band structure is given by [Moglestue, 1993; Jacoboni, 1989]

$$R_{im}(k) = \frac{8\pi n_i e^4}{k_s^2 \hbar q_0}(m_t^{*2} m_l^*)^{1/2} \gamma^{1/2}(E) \frac{1+2\alpha E}{1+4\sqrt{2}\gamma(E)(m_t^{*2} m_l^*)^{1/6}/\hbar q_0} \tag{14}$$

Where n_i is the impurity concentration, q_0 is the screening length and k_s is the dielectric constant of the material.

Electron-plasmon scattering

The electron-plasmon interaction Hamiltonian can be written in random phase approximation as (Di, 1991; Mansour, 1991)

$$H_{\text{int}} = \sum M_q (a_q c^+_{k+q} c_k + a^+_{-q} c^+_{k+q} c_k) \tag{15}$$

Here a_q^+, a_q and c_k^+, c_k are the creation and annihilation operators for plasmons and electrons, respectively. The matrix element

$$M_q = \sqrt{\frac{e^2 \hbar^3}{8\Omega \varepsilon m^{*2} \omega_p(q)}}.(2qk + q^2)/q \tag{16}$$

Where $\omega_p(q)$ is the dispersion relation for plasmons, q and k are the plasmon and electron momenta, respectively, e and m^* are the charge and effective mass of an electron, ε the background dielectric constant, and Ω the real-space volume. The first term in parentheses in equation 15 describes the plasmon absorption process which obeys the energy conservation law as

$$\varepsilon_{k+q} - \varepsilon_k = \hbar\omega_p(q) \geq 0 \tag{17}$$

Where ε_k is the energy of electron with momentum k. In a similar manner, the plasmon emission process, in accordance with the second term in parentheses in equation 15, is governed by the energy conservation law which can be written as

$$\varepsilon_k - \varepsilon_{k+q} = \hbar\omega_p(q) \geq 0 \tag{18}$$

Note that equation 17 describes the emission of plasmon with momentum -q. To impart a more conventional form to the energy conservation law, repalce the variable of summation q in terms governing the plasmon emission in equation 1 by -q. Then we can rewrite equation 15 as

$$H_{\text{int}} = \sum (M_q a_q c^+_{k+q} c_k + M_{-q} a^+_q c^+_{k-q} c_k) \tag{19}$$

The notation of equation 15 leads to the following form of the energy conservation law for the emission processes

$$\varepsilon_k - \varepsilon_{k-q} = \hbar\omega_p(q) \geq 0 \tag{20}$$

From the Fermi Golden rule, we can calculate the electron-plasmon scattering rates for emission W_e and absorption W_a

$$W_{e,a}(k) = \frac{2\pi}{\hbar}\int \frac{\Omega dq}{8\pi^3} \left|\langle f | H_{\text{int}} | i \rangle\right|^2 \times \delta[\varepsilon_{k'} - \varepsilon_k \pm \hbar\omega_p(q)] \tag{21}$$

Where k and k' are electron momenta in an initial state $|i\rangle$ and a final state $|f\rangle$, respectively. Here and further the upper signs in formulae correspond to the plasmon emission, whereas the lower ones do to the plasmon absorption. By using equation 15 and the energy conservation requirements in the forms of equations 18 and 20 which are consistent with this notation of H_{int}, equation 21 becomes

$$W_{e,a}(k) = \frac{2\pi}{\hbar}\int \frac{\Omega dq}{8\pi^3} M^2_{\mp q} \delta[\varepsilon_{k\mp q} - \varepsilon_k \pm \hbar\omega_p(q)] \times \{(N_q+1)_{em};(N_q)_{ab}\} \tag{22}$$

Where N_q is the Bose-Einstein distribution function for plasmons. The integration bounds with respect to q are defined from the following conditions

$$\begin{aligned} \omega_p(q) &\leq \hbar kq/m^* \mp \hbar q^2/2m^* \\ \omega_p(q) &\geq \hbar k_f q/m^* + \hbar q^2/2m^* \end{aligned} \tag{23}$$

Where k_f is the electron momentum at the Fermi surface.

RESULTS

The electron-plasmon scattering is included only in the low effective mass Γ valley. So, we have just taken into account the temperature and electron concentration dependence of the electron mobility in the Γ valley, which arises due to the different scattering mechanisms. The electron mobility as a function of temperature in bulk ZnO and SiC materials for various types of scattering mechanisms such as ionized impurity, acoustic phonon via

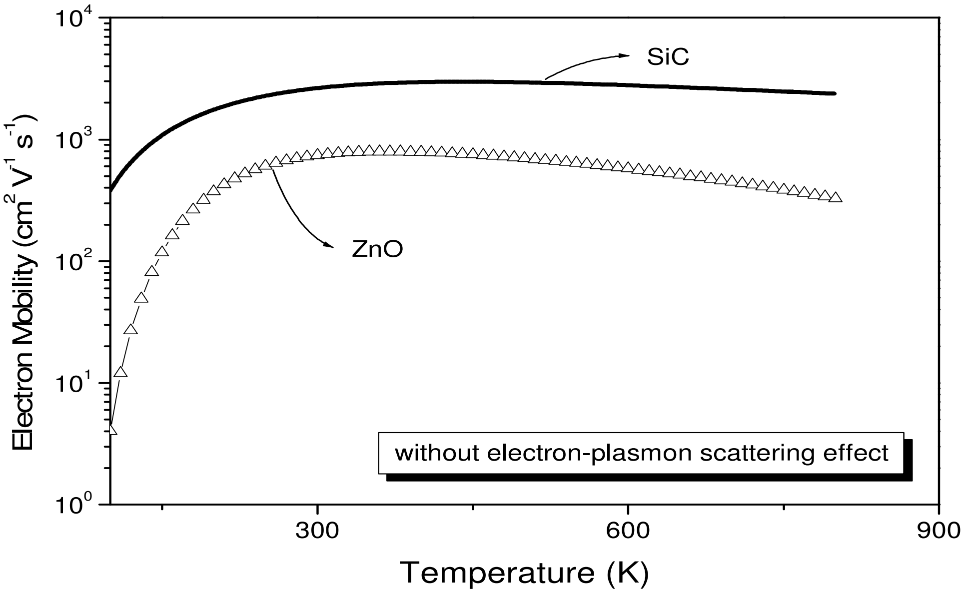

Figure 1. Calculated electron mobility in bulk ZnO and SiC as a function of temperature assuming a donor concentration of 10^{22} m^{-3} without the electron-plasmon scattering.

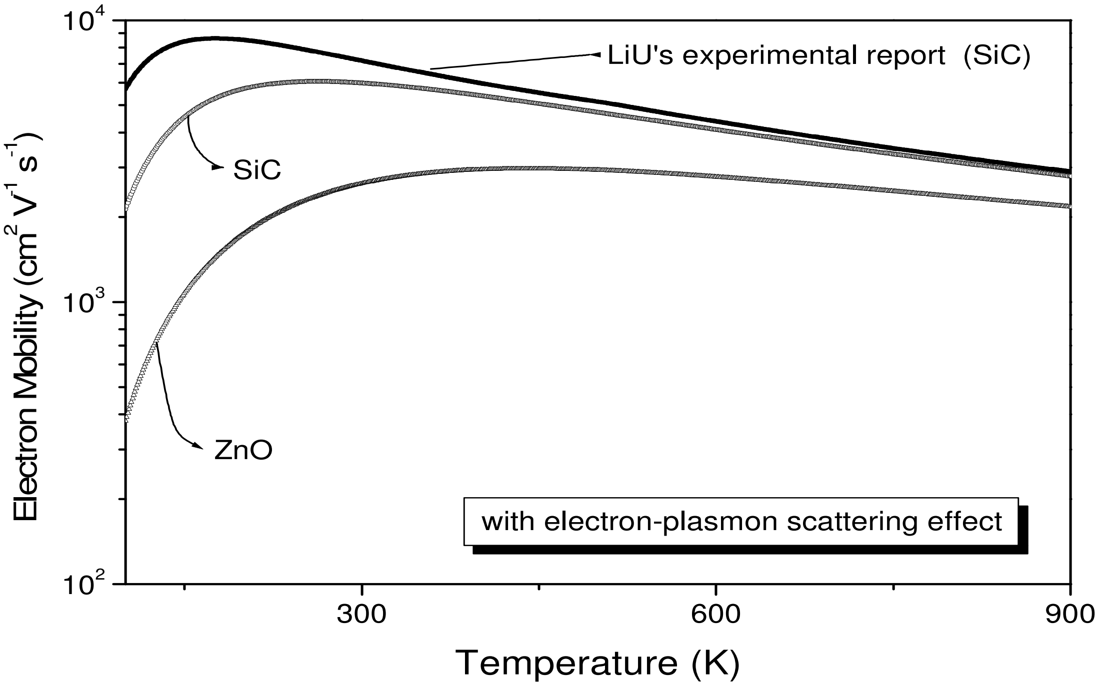

Figure 2. Calculated electron mobility in bulk ZnO and SiC as a function of temperature assuming a donor concentration of 10^{22} m^{-3} with the electron-plasmon scattering.

deformation potential and polar optical phonon but without electron-plasmon scattering effect is shown in Figure 1.

As it is seen, the decrease in electron mobility at low temperature is caused in part by ionized impurity scattering versa the step reduction at higher temperature is due to large optical phonon scattering.

Figure 2 shows again the variation of electron mobility

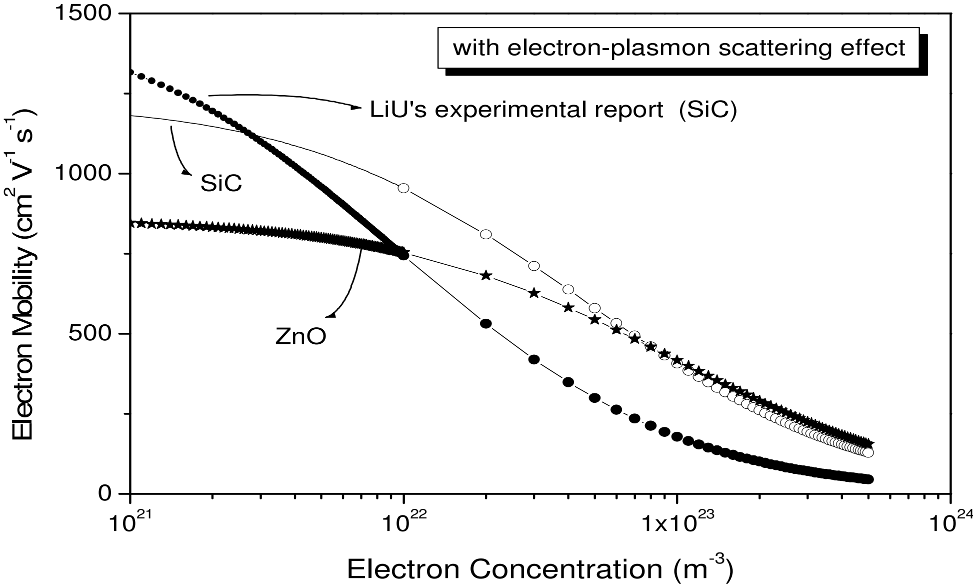

Figure 3. Calculated low-field electron drift mobility in bulk ZnO and SiC as a function of different donor concentration at room temperature including the electron-plasmon scattering in comparison with experimental report.

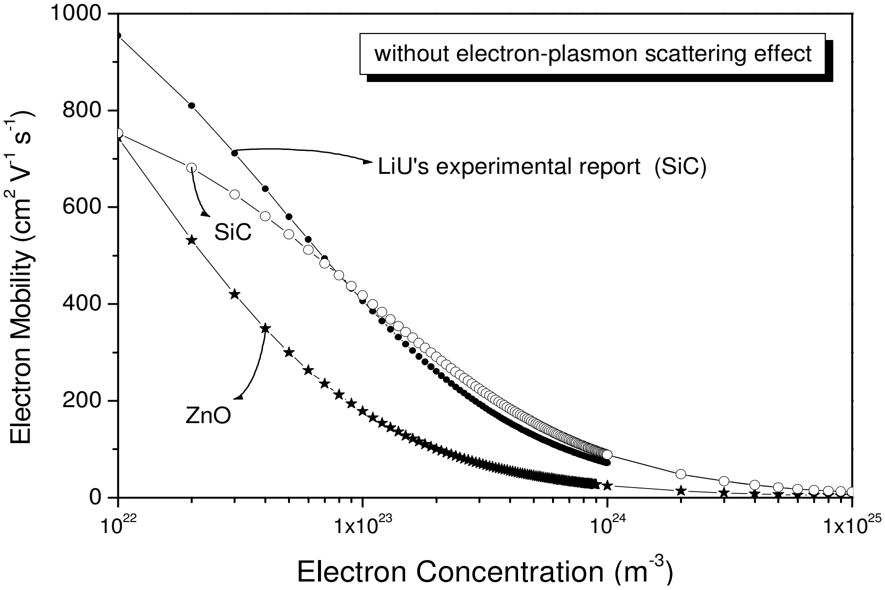

Figure 4. Calculated low-field electron drift mobility in bulk ZnO and SiC as a function of different donor concentration at room temperature without the electron-plasmon scattering in comparison with experimental report.

as a function of temperature adding electron-plamon scattering effect. As it can be seen, inclusion of the electron-plasmon scattering leads to the effecive heating of the hot-electron system. The calculated results for SiC are in comparison to the Liu et al. (2000) (experimental report which shows good agreements).

Figures 3 and 4 show the calculated variation of the electron mobility as a function of the donor concentration in bulk ZnO and SiC crystal structure at room temperature with and without inclusion of electron-plasmon scattering effect, respectively. It can be seen that in both cases there is a fair agreement with the Liu et al. (2000)

(experimental report). Also the figures show that the mobility does not vary monotonically between donor concentrations of 10^{21} and 10^{24} m^{-3} due to the dependence of electron-plasmon scattering on donor concentration, but shows a maximum near 10^{21} m^{-3} for both structures.

Conclusion

The computed low-field electron mobility in bulk ZnO and SiC materials show that SiC has superior electron transport properties. It is shown that including the electron-plasmon scattering effect increase the electron mobility of two structures by 10%, and Ohmic mobility drops by the same percent. This is caused by combined effects of effective heating of electron gas by electron-plasmon scattering and predominantly forward peaked momentum relaxation for all electron momentum.

ACKNOWLEDGEMENTS

I would like to thank M. G. Paezi for her useful comments.

REFERENCES

Hamdani F (1997). High field electron transport properties in ZnO, Appl. Phys. Lett. 70: 467.

Look DC (2005). Monte Carlo study of electron transport in SiC, Semicond. Sci. Technol. 20 pp S55.

Kim SH, Lee JS, Choi HS, Lee YH (1999) Crystal growth of Zno and SiC, IEEE Electron Device Lett. 20: 113.

Tsukazaki A, Ohtomo A, Onuma T, Ohtani M, Kawasaki M (2005). Nat. Mater. 4: 42

Makino T, Segawa Y, Ohtomo A (2001). Appl. Phys. Lett. 78: 1237.

Bellotti E, Doshi BK, Brennan KF (1999). J. Appl. Phys. 85 : 916.

Look DC, Reynolds DC, Sizelove JR, Harsch WC (1998). Solid State Commun. 105: 399.

Chen Y, Bagnall DM, Koh HJ, Park K T, Zhu Z Q , Yao T (1998).J. Appl. Phys. 84: 3912.

Moglestue C (1993). Monte Carlo Simulation of Semiconductor Devices, Chapman and Hall.

Jacoboni C, Lugli P (1989). The Monte Carlo Method for semiconductor and Device Simulation, Springer-Verlag.

Ridley BK (1997). Electrons and phonons in semiconductor multilayers, Cambridge University Press.

Chattopadhyay D, Queisser HJ (1981). Review of Modern Physics, 53, part1

Di K, Brennan K (1991).J. Appl. Phys. 69: 3097.

Mansour N, Di K, Brennan K (1991). J. Appl. Phys. 70 pp 6854.

Liu Y, Gorla CR, Liang S, Emanetoglu N, Wraback M (2000).J. Electron Mater. 29: 69.